International Journal of Nanoelectronics and Materials
IJNeaM
ISSN 1985-5761 | E-ISSN 2232-1535

Effect of Electrospinning Parameters on the Morphological and Thermal Properties of ABS/ENR Electrospun Fibres

Mahathir Mohamed[a,b], Abu Bakar Sulong[a]*, Rosiah Rohani[c], Mohammad Iqbal Shueb[a], Mohd Sofian Alias[a] and Mohd Hamzah Harun[a]

[a]*Department of Mechanical and Manufacturing Engineering, Faculty of Engineering and Built Environment, Universiti Kebangsaan Malaysia, Bangi, 43600 Selangor, Malaysia*
[b]*Radiation Processing Technology Division, Malaysian Nuclear Agency, Bangi, 43000 Kajang, Selangor, Malaysia*
[c]*Department of Chemical and Process Engineering, Faculty of Engineering and Built Environment, Universiti Kebangsaan Malaysia, Bangi, 43600 Selangor, Malaysia*
∗Corresponding author. Tel.: +60-13-332-0909; fax: +60-38925-9659; e-mail: abubakar@ukm.edu.my

Received 8 March 2023, Revised 5 October 2023, Accepted 25 October 2023

ABSTRACT

The electrospun of the Acrylonitrile-butadiene-styrene (ABS) blend with epoxidized natural rubber (ENR) is fabricated using the electrospinning technique. Research shows that ABS/ENR electrospun fibres have not been studied. The effects of electrospinning parameters were investigated to determine a significant effect on the microstructure, surface roughness, fibre diameter, and fibre distribution of the electrospun membranes. Sample preparation is made straightforwardly by dissolving ABS and ENR in acetone solvent using a magnetic stirrer. In this research, there are two solution parameters being studied: the ABS/ENR solution concentration (15 to 25 wt.%) and the ratio of ENR (100:0, 70:30, 50:50). Meanwhile, process parameters that are being studied are applied voltage (15 kV to 30 kV) and distance from syringe tip to collector (5cm to 15cm). FTIR results showed that hydrogen bond interaction occurs between ABS and ENR. According to the SEM images, micrometre and sub-micrometre fibres with a smooth surface and bead formation were produced at a concentration of 25%, a ratio of 70:30, a voltage of 30kV, and a distance of 15cm. The diameter of electrospun fibres increases with increasing solution concentration, ranging from 400 nm to 4.5 µm. The diameter of the electrospun fibres decreased with the addition of ENR, increasing voltage, and tip-to-collector distance. TGA results showed that ABS/ENR blends gave higher degradation temperature (393.7°C) than pure ABS (368.8°C), which enhanced thermal stability.

Keywords: *Electrospinning, Epoxidized natural rubber (ENR), Electrospun membranes, Sub-micrometre, Thermal stability*

1. INTRODUCTION

Electrospinning, a widely used technology to prepare nonwoven fibre, has gained much interest in the scientific community. The process involves natural and synthetic polymers as raw materials, and the nonwoven fibres are produced as a result of the electrostatic force between the polymer solution and the collection plate [1-2]. Electrospun nanofibres produce a stable range of radius, from several nanometers to several microns. Nanofibres produced by electrospinning have numerous advantages, such as large specific surface area and porosity, and wide ductility of size and shape. Furthermore, the components and the formation design of the nanofibres can be controlled extensively [3]. Electrospinning is deemed to be a well-known and versatile technology for the manufacture of fibre materials, such as composite fibres, porous structure fibres and polymer fibres [2,4]. There is a wide-ranging array of potential applications of the polymer nanofibres fabricated by electrospinning, such as filtration, material enhancement, insulation isolation, and energy storage [4-6].

In recent years, the production of electrospun biodegradable fibres has garnered the scientific community's interest. However, limited studies have been conducted on producing elasticated fibres using renewable raw materials. In 2009, Sithornkul and Threepopnatkul performed the first study on the electrospinning of NR as part of their main investigation into the electrospinning of NR/ABS blends in tetrahydrofuran (THF). They investigated the effect on the morphology of the fibres produced by electrospinning when the concentration of ABS as well as the distance between the collector and needles, were varied. The diameter of the fibres produced varied from a range of 5.8 µm to 23 µm [7]. In another research published in 2016, electrospun fibres were created by combining an epoxidized natural rubber-25 (ENR-25) solution with crystalline grade polylactic acid (PLA) and a graft copolymer compatibilizer (ENR-g-JM). The smooth fibres' diameter ranged from 0.5 µm to 7 µm. Although the ENR-25 solution was not favourable to the electrospinning process, the fibres could be produced over a wide span of operating conditions due to the addition of PLA [6].

Meanwhile, the PVC/natural rubber blend at a 16 wt.% concentration was successfully produced by

electrospinning. Adding natural rubber to the process decreases the diameter of the fibres and the degradation temperature. Electrospun fibres produced with the inclusion of liquid epoxidized natural rubber acrylate (LENRA) had the smallest diameter and highest degradation temperature, which can be attributed to the presence of epoxy and acrylate groups [8].

Furthermore, the use of NR as a natural polymer is expanding because of its outstanding biocompatibility, biodegradability, and environmental friendliness. In contrast, the effect of NR in the blend of PLA was shown to increase in diameter when NR content was increased. The electronic paramagnetic resonance (EPR) technique was used to confirm that incorporating NR enhanced the amorphous phase mobility in PLA/NR fibres and was introduced at two different temperatures of the radical probe (T = 50° and 70° C). In comparison to PLA alone, the addition of 15% wt NR multiplied the elongation value at the break by a factor of 3.5 [9]. Epoxidized natural rubber (ENR), a chemically altered form of cis-1,4-polyisoprene rubber, has recently been employed as a plastic toughening agent. The remarkable interaction between PLA and ENR increases its impact strength when 10 wt.% ENR is added to the PLA matrix. Liquid epoxidized natural rubber (LENR), a degraded structure of the ENR, has a reduced molecular weight and a shorter chain due to the chain scission of the polyisoprene backbone [10-11]. LENR is more advantageous than ENR in producing numerous products as it is easier to process and requires less energy. Moreover, the lower molecular weight means LENR can be modified easily. It was reported in studies that unsaturated polyester resin (UPR) modified with LENR has better and improved mechanical properties compared to liquid natural rubber-unsaturated polyester resin (LNR-UPR) due to the excellent interaction between UPR and LENR [12].

Thus, producing electrospun fibres only using LENR is challenging and unattainable in our investigation. From the literature, it was found that LENR should be combined with other polymeric components that serve as a binder. Acrylonitrile-butadiene-styrene (ABS), a copolymer consisting of acrylonitrile, butadiene, and styrene, is a valuable and often used material in industries due to its exceptional physical and mechanical qualities, such as impact resistance and toughness. The preparation of ABS includes the polymerization of acrylonitrile-block-styrene with polybutadiene, and a polar nitrile group strengthens the resulting polymer chains.

ABS is made of polystyrene and polybutadiene, which make it stiff like plastic and flexible like rubber. These properties have made ABS a viable material for manufacturing products such as lego bricks, automobile console boxes, and safe transport containers [13]. The ABS copolymer is well-studied and has also been used for various applications. However, the construction of ABS fibres, especially from several hundred nanometres to micrometres, has yet to be explored. The ABS/LENR electrospun fibres are expected to be used in more applications accounting for the beneficial physical and mechanical properties of the ABS/LENR blend. These blends have potential applications in filtration, wound dressing, tissue engineering, and drug delivery benefiting from the high surface area to volume ratios [13-15]. Operating parameters, such as the solvent, concentration of the polymer solution, flow rate, ratio of materials, working distance and voltage of the electrospinning process, can control the morphology and size of the ABS/LENR fibres.

This study aimed to develop a novel nonwoven fibrous-based ABS/LENR blend using an electrospinning technique. The surface of this fibrous membrane was analysed using a scanning electron microscope (SEM), which revealed images of electrospun threads that were dependent on carefully controlled electrospinning conditions. The morphology acquired by SEM revealed the surface and thermal characteristics of the electrospun fibrous membrane. The novelty of this paper is that micro-nanofibre layers were produced using electrospinning and LENR as an additive in ABS solution to improve hybrid material properties. The compatible blend of LENR and ABS solution was investigated by thermal gravimetry analysis (TGA) and Fourier transform infrared spectroscopy (FTIR) respectively.

2. METHODOLOGY

2.1. Materials

Acrylonitrile Butadiene Styrene (Toyolac ABS) was used as the host polymer due to its high thermal and mechanical properties. Epoxidized natural rubber (ENR, 50 mol % conversion) was used as the modifier supplied by Guthrie Malaysia. Degradation of ENR via UV irradiation to form low molecular weight liquid epoxidized natural Rubber (LENR). LENR molecular weight was between 4.0×10^4 and 8.0×10^4, which was determined by gel permeation chromatography (GPC). Acetone, as a solvent, was purchased from Sigma Aldrich Chemical Co. The ABS particles were dissolved at room temperature (25°C) in the acetone using a magnetic stirrer with 24 hours of stirring. Degraded ENR in solution was mixed with ABS solution using a magnetic stirrer at room temperature for 5 hours to get a homogenous blend.

2.2. Electrospinning

Electrospinning was carried out using a custom-built electrospinning apparatus that included a high-voltage power source (ES30P-5W, Gamma High Voltage Research), a syringe pump (KD Scientific), and a flat collector. A syringe pump with a 20-ml syringe combined with an 18G metallic needle (inner diameter 0.9 mm) was used to release the prepared solution in the electrospinning process. The electrospinning process was conducted at room temperature with a flow rate of 4 mL/h. Electrospinning parameters such as concentration, ABS/ENR ratio, voltage, and distance were studied. The concentration of the solution varied between 15% and 25%. The voltage setting range is between 15 and 30 kV. ABS/ENR ratios are 100:0, 70:30, and 50:50. The tip-to-collector distance was fixed at 5 cm, 10 cm, and 15 cm. During the electrospinning process, randomly oriented electrospun fibre mats were prepared and collected on flat

aluminium foil. Different parameters of electrospinning and the size of electrospun fibres are listed in Table 1.

2.3. Characterization

The infrared (IR) spectra of the ABS, ENR, and ABS-LENR were recorded using the Fourier transform infrared spectrometer (FTIR) (Perkin Elmer Spectrum 2000). The samples underwent five scans ranging from 4000 to 500 cm^{-1} with a resolution of 4 cm^{-1}. The nanofibers' surface morphologies were characterised using a scanning electron microscope-FEI Quanta400 at 500x and 2000x magnification. The experiments were conducted in high vacuum mode under a voltage of 20 kV. The samples were coated with a thin coating of gold using a sputter coater (model SC 500) in an inert gas (Argon) atmosphere at 0.1–0.5 torr. SEM examinations were carried out on the fibre membrane samples. The fibre diameter was averaged from the measurement of 100 randomly selected fibres using Image J 1.48 software. At a specified temperature, samples' temperature resolution and percentage weight loss were determined using the TGA Q500 TA instruments model. During the analytical run, the samples experienced degradation. An analysis was done on fibre membrane samples heated at 10°C per minute from room temperature up to 700°C. For this investigation, a sample weight of 3 mg was used. The different ratios of natural rubber employed provide other temperature resolutions.

Table 1 Sample with various parameters and average diameter of fibres

	Concentration (%)	Ratio (ABS/ENR)	Voltage (kV)	Distance (cm)	Fibres diameter (μm)
S1	15	90:10	15	15	0.67±0.22
S2	20	90:10	15	15	1.05±0.33
S3	25	90:10	15	15	2.29±0.84
S4	20	100:0	15	15	1.72±1.00
S5	20	70:30	15	15	1.57±0.68
S6	20	50:50	15	15	0.89±0.32
S7	20	70:30	15	15	1.18±0.41
S8	20	70:30	20	15	0.89±0.30
S9	20	70:30	30	15	0.95±0.37
S10	20	70:30	20	5	1.02±0.33
S11	20	70:30	20	10	0.77±0.34
S12	20	70:30	20	15	0.69±0.36

3. RESULTS AND DISCUSSION

3.1. Fourier Transform Infrared (FTIR) Spectra

For comparison, IR spectra for ABS, ENR, and ABS/ENR electrospun membranes are shown in Figure 1. Frequent peaks are shared by the ENR and ABS, especially in the fingerprint region. The infrared spectrum of ENR showed peaks at 2920 and 2852 cm^{-1}, which were assigned to the asymmetrical and symmetrical stretching vibration of the methylene group, respectively. The absorption peaks at 877, 905, 1067, 1251, and 1378 cm^{-1} for the asymmetric stretch of C-O, C-O stretch, and symmetric C-O indicated the presence of an epoxy group in the ENR spectrum. The epoxy group in ENR gives the material characteristics like resistance to oil and organic solvents, air permeability, damping, good interaction with polar plastics, and resistance to wear. The epoxy group was added to natural rubber through a process called epoxidation. This process uses acid performic and hydrogen peroxide, and this reaction involves the addition of oxygen atoms into unsaturated carbon double bonds in the NR chains [16-17]. The ENR spectrum also revealed a slightly broad O-H stretching band (3600-3100 cm^{-1}) resulting from partial cleavage of oxirane into diols during degradation under UV exposure.

Meanwhile, the infrared spectrum of ABS showed absorption peaks at 2238 cm^{-1} ascribed to nitrile. Some characteristic peaks of ABS can be observed at 1602 and 1494 cm^{-1} are related to the ring modes of styrene and the peaks at 967 and 911 cm^{-1} belong to the butadiene component [18]. Multiple peaks were also detected in the range of 2000–1500 cm^{-1}, attributed to the C═C and C═O bonds. Additionally, sharp and strong stretched peaks were observed within the range of 1500 –1000 cm^{-1}, due to the presence of C–C, C–O, C–N, C–N–H, and ester groups [19-20].

In the ABS/ENR spectrum, there are several peaks within the precise wavenumber; there are no additional peaks, but there are changes in peak widening and peak shifting. The ABS/ENR spectrum displayed characteristic peaks for the isoprene units at wave numbers 1663 and 835 cm^{-1}, assigned to the stretching of C=C bond and out-of-plane deformation of ═C-H, respectively. We can see in the

spectrum the reduction in the absorption of the peak at 835 cm^{-1} for the double bonds C=CH, suggesting a hydrogen bonding interaction at the interface by the nitrile group. The decreasing relative intensity of the peak at spectral region 2851 - 2920 cm^{-1} reveals a decline in the concentration of C-H in ABS/ENR, while the broad peak at 3620 cm^{-1} can be attributed to the effect of hydrogen bonding [21-23]. Due to the presence of hydrogen bond acceptors in both ABS and ENR, such as C=O, C-OH and CN, both compounds would exhibit strong hydrogen bonding simultaneously, resulting in high dispersion and miscibility[24]. The spectra make it clear that there is no possibility of a chemical reaction or of a covalent bond taking place. As a result, the physical interactions that occur during the blending process, such as the Van der Waals force and hydrogen bonding, play a vital role.

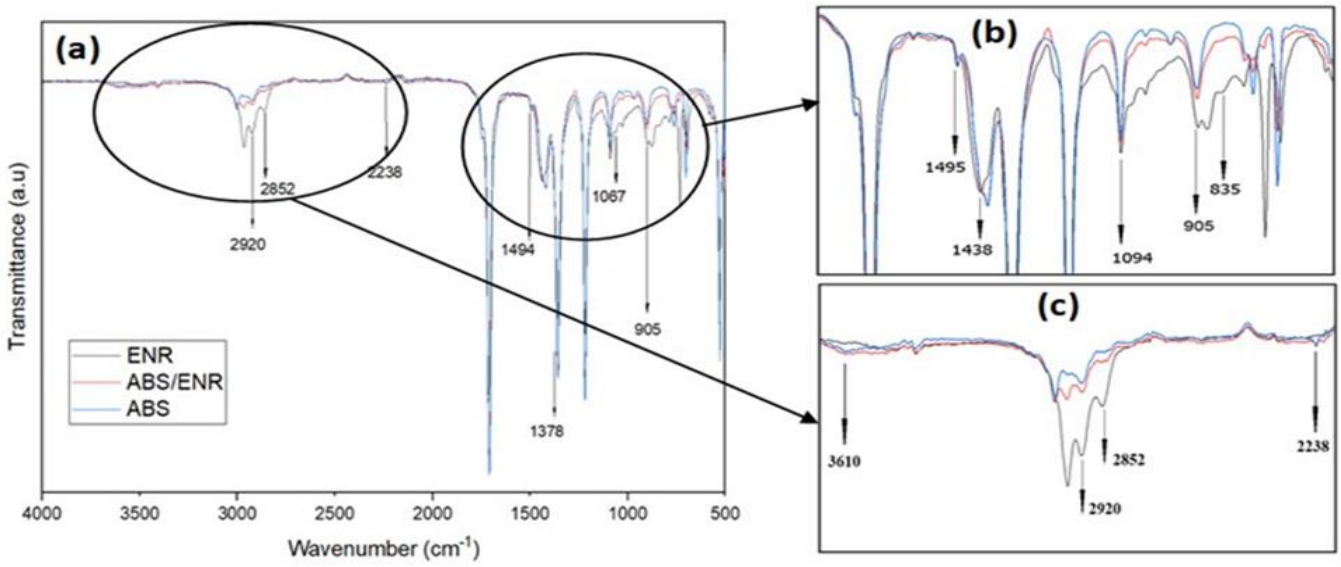

Figure 1 FTIR spectra of the ENR, ABS-ENR and ABS

3.2. FTIR spectra of the ENR, ABS-ENR and ABS

In this study, continuous ABS/ENR fibres were electrospun successfully from the ABS/ENR/acetone solutions in the concentration ranges between 15%, 20%, and 25%. Adding low molecular weight ENR could enhance flexibility and act as a plasticizer for ABS fibres. To determine the effect of concentration on electrospun fibre formation, other factors such as ENR ratio, voltage, and distance were kept constant (Table 1). Figure 2 (a, b, c) shows that beaded fibres were formed at a 15% ABS/ENR concentration, whereas continuous and smooth fibres were produced at a 20% and 25% ABS/ENR concentration, respectively. As the ABS/ENR solution concentration was increased, the beads gradually disappeared, and the form of the beads changed from sphere to spindle-like.

Figure 2 (a1, b1, c1) shows that when the solution concentration increases, the average diameter of electrospun fibres becomes more prominent, and the fibre size distributions become broad. The size distribution of ABS/ENR electrospun fibres was determined using a statistical analysis of 100 fibres. The average diameter was 0.67 µm at 15%, 1.05 µm at 20%, and 2.29 µm at 25% concentration, respectively. At a higher concentration, the viscosity of the ABS/ENR solution increases, and the number of polymer molecules also increases. It creates more entanglement of polymer chains [25-26]. The change in the solution viscosity can be attributed to the following results: bead formation at low polymer concentration; and an increase in the diameter of the fibres as the concentration of the solution increases. The number of polymer (ABS) chain molecules entangled in a solution relates to the solution viscosity. Low-viscosity solutions have low viscoelastic force and the electrospinning process stretches the electrospinning jet due to electrostatic and columbic repulsion forces. The unequal forces cause a partial split in the jet.

Nuge et al. reported that an increase in polymer concentration in a solution causes a rise in viscosity, resulting in a greater viscoelastic force. This improved force minimizes the partial disintegration of the jet. There is also an increase in the polymer chain entanglement as the concentration of the solution increases, which helps the solvent molecules spread over the entangled polymer molecules. This phenomenon produces smooth fibres, increases the diameter of the fibres, and improves the fibres' uniformity [27]. As discussed above, it has been found that the increase in the diameter, and uniformity of the ABS/ENR fibres, as a result of the progressively increasing viscoelastic force, restrict the stretching influence of electrostatic and columbic repulsion forces on the fibres.

Furthermore, as mentioned by Zulfi et al. the surface tension of the solvent (acetone) has a significant impact on the morphologies of ABS/ENR electrospun fibres. Decreasing the surface tension of the solution (high concentration) causes beads to disappear gradually. The

lower the surface tension, the greater the chance that smooth ABS/ENR fibres can be obtained from a particular solvent [28-29].

viscosity. Meanwhile, the fibre size distribution and average fibre diameter show some improvement in terms of size (Figure 3a1,b1,c1). It is clear that at a ratio of 100:0

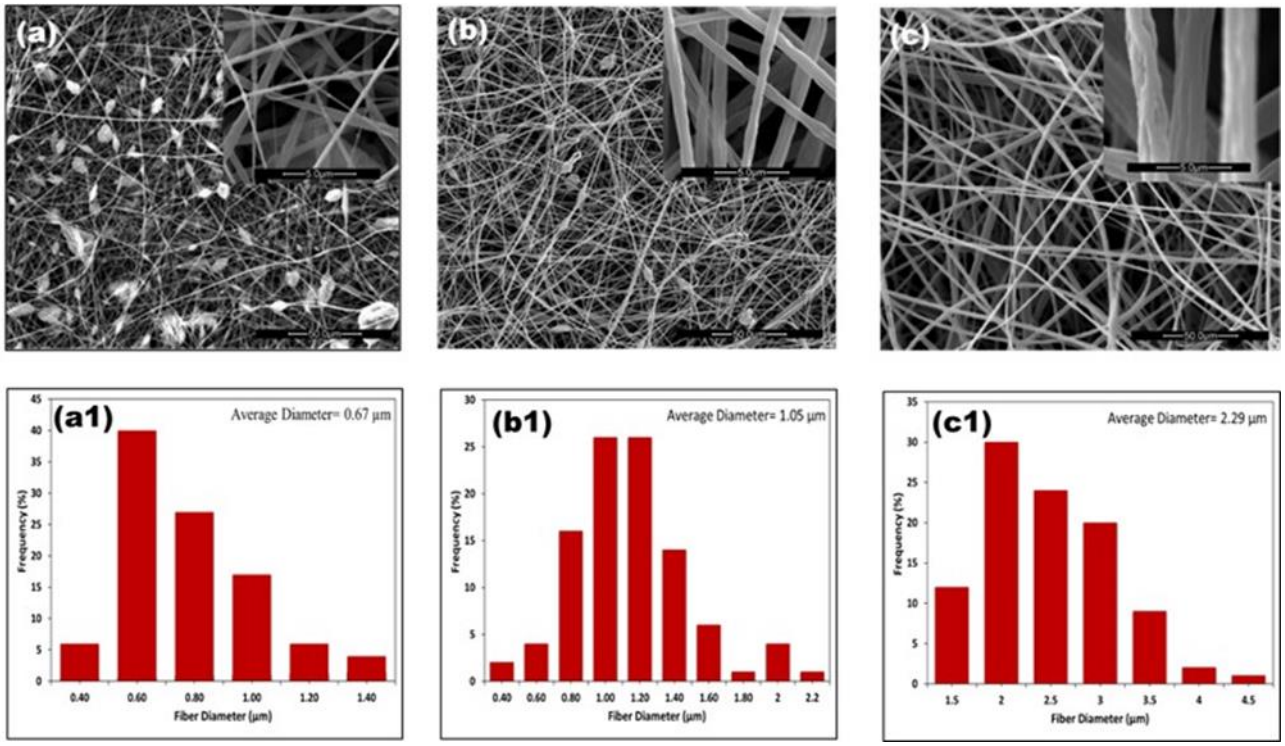

Figure 2 SEM images of membrane with concentration of (a) 15wt%, (b) 20wt%, (c) 25wt% and fibres size distribution (a1,b1,c1)

3.3 Effect Of ENR Ratio

To study the influence of ENR on the morphology of ABS/ENR electrospun fibres, the ABS/ENR blend ratios of 100/0, 70/30, and 50/50 were analyzed. Figure 3(a, b, c) shows the morphology of ABS/ENR electrospun fibres after different ratios of epoxidized natural rubber were added (other parameters are set to be constant at a concentration of 20 wt.%, the voltage of 15 kV, needle tip-to-collector distance of 15cm). The diameter size of electrospun fibres was calculated using 100 fibres picked at random. The micrograph demonstrates the formation of long continuous and smooth electrospun micro nanofibres at 100:0 and 70:30 ratios (ABS: ENR). The changes in fibre form are comparable to the effect of concentration, which significantly affects micro-nanofibres' morphology. As the ENR increased, a spindle-like bead formation could be noticed on the electrospun fibres prepared from the ABS/ENR (50:50) solution (Figure 3c). Bead fibres are "by-products," which are common in electrospinning. The instability of the sample solution jet, electrospinning net charge density, solution viscosity, and solution surface tension have all been linked to the formation of beaded fibres [5].

The more extensive content of ENR could increase well dispersion, improve compatibility and provide good interfacial adhesion between two blend components [30]. This is because the ENR might function as a compatibilizer between the two components of blends and will have a modest influence on the viscosity of the solution mix. Therefore, this result shows that many bead fibres could be produced at a larger ratio of ENR due to the decreasing (ABS: ENR), the diameter of electrospun fibres is greater than that of ENR-containing fibres. The average fibre diameters gradually decreased from 1.72 µm to 0.89 µm for the 100:0 (ABS/ENR) and 50:50 (ABS/ENR) ratios. At higher ENR content, it shows a broad fibre size distribution, but it shows the opposite result at low ENR, which is narrower. Thus, a rubber ratio of 70:30 gives a perfect fibre outcome when various factors are fixed. According to this research, the ideal fibres are free of beads and have a smooth surface. The electrospun fibres generated are appropriate for various applications, including water, air, and sensors.

3.4 Effect of voltage

At various voltage levels, Figure 4 displays the morphology of the beads and the average diameter of the electrospun ABS/ENR fibres. Three applied voltages of 15, 20, and 30 kV were independently applied for electrospinning ABS/ENR solutions while leaving all other parameters constant. Figure 4(a, b) shows that the average fibre diameter decreased as the applied voltage increased. At 15kV and 20kV, the average diameters are 1.18 µm and 0.89 µm. Figure 4c shows that a 30 kV applied voltage caused the ABS/ENR solution to eject in a more fluid jet, resulting in an enhanced fibre diameter of 0.95 µm. From the data obtained, it is essential to note that while there was a wide distribution of the diameters of the ABS/ENR fibres when the applied voltage was 15 kV, the distribution was relatively narrow at the applied voltage of 20 kV and was broad again at the applied potential of 30 kV (Figure 4a1,b1,c1).

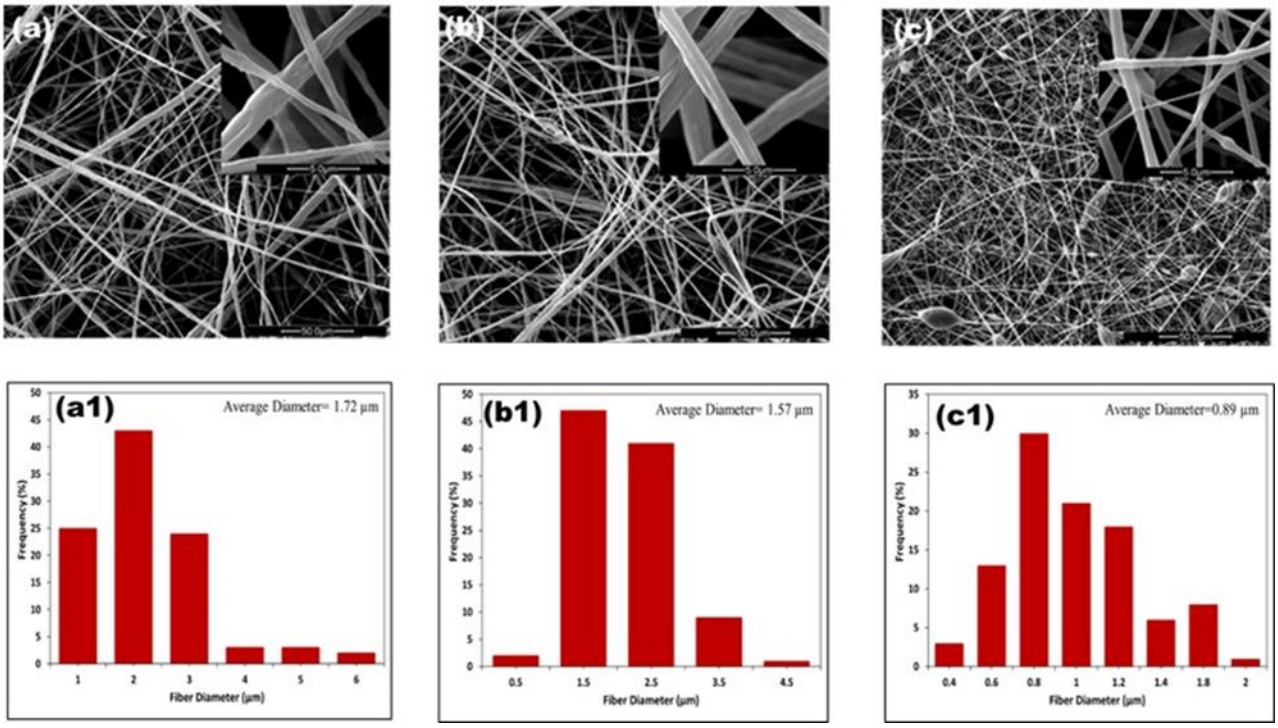

Figure 3 SEM images of membrane with different ratio of ABS/ENR (a) 100:0, (b) 70:30, (c) 50:50 and fibres size distribution (a1, b1, c1).

The impact of applied voltage on the diameters of the ABS/ENR fibres can be described in terms of the relationships between the three principal forces (the Coulombic, the viscoelastic, and the surface tension), which affect the fibres' diameters. Compared to the surface tension at low voltages (15 kV), the Coulombic force was not strong enough, resulting in ABS/ENR electrospun fibres with high diameters and big beads along the threads. The three forces were well-balanced at a modest applied voltage (20 kV), resulting in a limited dispersion of the fibres' diameters. Huan et al. used electrospinning to create PS/DMF nanofibres and examined the influence of applied voltage on fibre sizes [32]. They discovered that applying a low voltage had the same impact as increasing it, which led to the production of as-spun fibres with large diameters and the presence of big beads along the fibres. The consequent increase in the applied voltage (30 kV) results in a more prominent Coulombic force than the viscoelastic force. This increases the probability of rupturing the over-stretched charged jet during its passage to the target.

Moreover, the charged jet can fly faster to the grounded target with a larger applied voltage (30 kV). Therefore, there is less time available for the solvent to evaporate. The charged jet retracts, and part of the jet is neutralized, resulting in more oversized but irregular fibres. Tungprapa et al. successfully synthesised cellulose acetate (CA) in acetone-DMF at 8, 12, 16, and 20 kilovolts voltages. They discovered that as-spun fibres increased with increasing applied EFS (electrostatic field strength), from 0.23 µm with an applied EFS of 8 kV to 0.42 µm with an applied EFS of 20 kV [31-32]. Thus, an optimal voltage is essential to obtain thinner electrospun fibres after considering the differential effects.

3.5 Effect of distance

The distance between the tip of the syringe and the collector is another critical component in determining electrospun fibres' diameter and morphologies. Figure 5 depicts the morphology of the effect of distance on the diameter size and uniformity of electrospun fibres. Figure 5c displays the smallest diameter size of electrospun fibres, about 0.69µm compared to Figure 5a and 5b (1.02µm and 0.77µm). Furthermore, it shows a narrow fibre size distribution at the highest distance (15cm) compared to the low distances of 5cm and 10cm (Figure 5a1, b1, c1). The distance between the needle tip and the collector impacted the deposition time, solvent evaporation rate, and interval instability [33]. For the extremely short distance, the electrical field became quite strong, which enhanced the instability of the jet solution and permitted many jets to emerge from one nozzle, leading to the development of bead fibres. In this study, it was demonstrated that this is accurate, following the theory suggested, that electrospun ABS/ENR fibres exhibit a bead-like shape when observed from a distance of 5 and 10 centimetres.

Meanwhile, an increase in the distance between the tip and the collector led to the ABS/ENR fibres production without the beads' presence. While in flight, electrospun ABS/ENR fibres are generated as the polymer solution hardens and the solvent is depleted from the surface. The thinning time is extended with increasing spinning distance, and if the polymer does not solidify yet, the average diameter of the fibres will be lower [26,28]. This study yields the same results as Matabola and Moutloali's research, which produced fibre that is uniform and smooth [33]. Furthermore, the electric field must be strong enough to push the polymer jet long distances while considering adverse effects such as air resistance and localized charge

concentrations. Therefore, increasing the distance by 15 cm significantly affects ABS/ENR fibre morphology because the long distance enables more time for the solvent to evaporate and permits the charged fluids to split more.

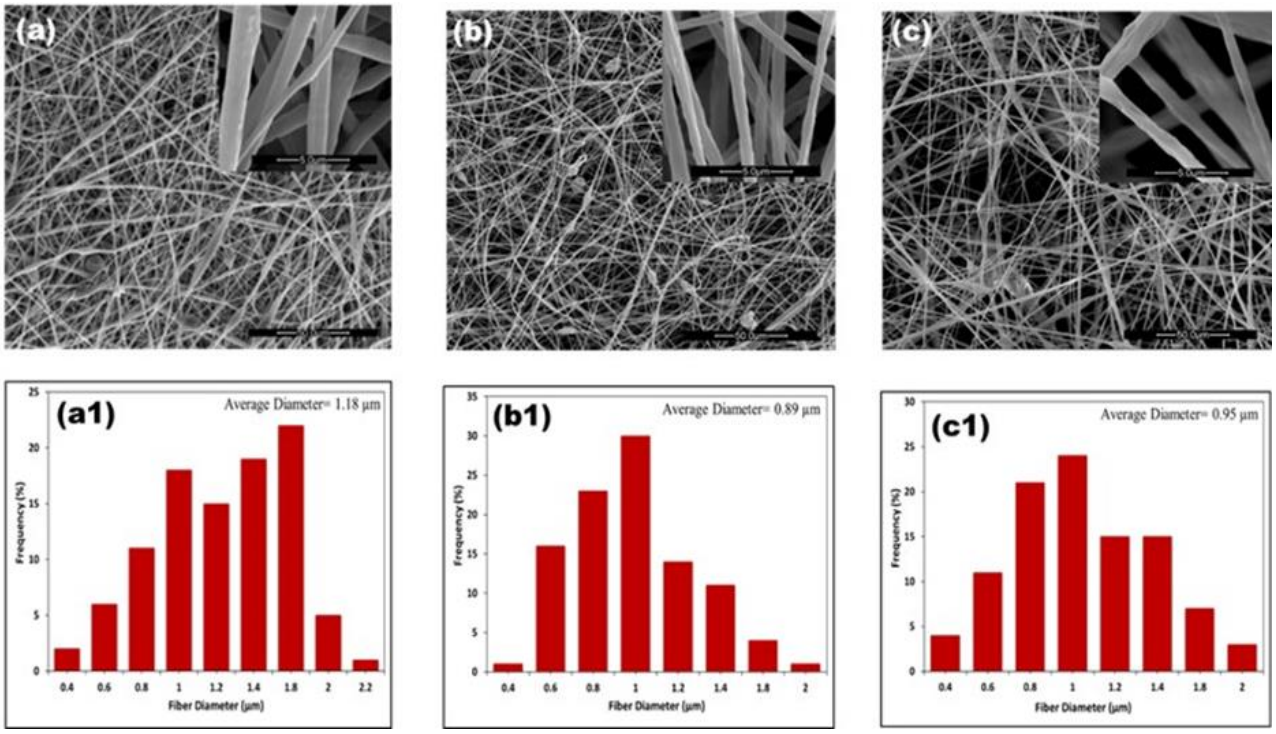

Figure 4. SEM images of membrane at different voltage (a) 15kV, (b) 20kV, (c) 30kV and fibres size distribution (a1, b1, c1).

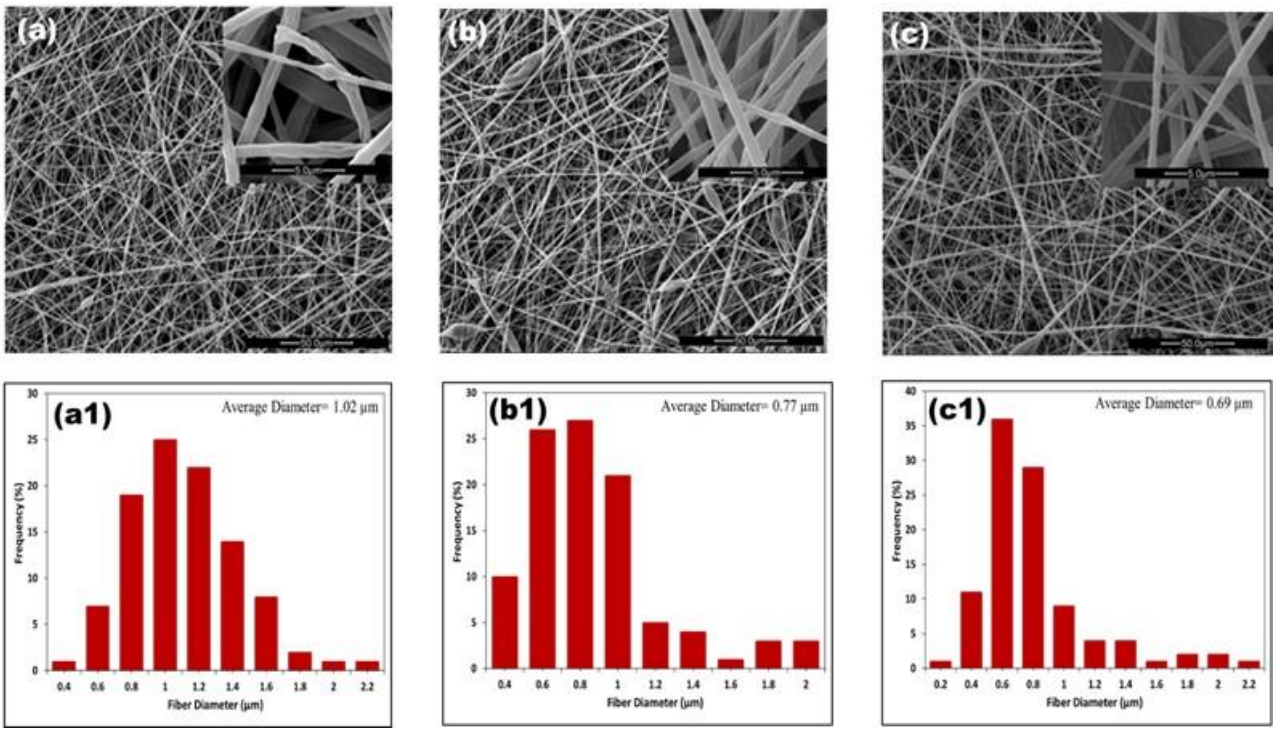

Figure 5. SEM images of membrane at different distance (a) 5cm, (b) 10cm, (c) 15cm and fibres size distribution (a1, b1, c1).

3.6 Thermal Stability

The TGA curves for ABS/ENR electrospun fibres are shown in Figure 6. The presence of ENR in the fibres affected the weight loss temperature. The results indicate that when electrospun fibres containing 10%, 30%, or 50% ENR are compared to pure ABS, the onset temperature or point of thermal degradation is shifted upward with increasing ENR loading. The onset temperature increases from 368.8°C to 393.7°C when 30% ENR is added to the mixture. The increase in degradation temperatures implies that the ABS/ENR blends have improved thermal stability with the addition of ENR. The increased thermal stability of ABS/ENR blends is attributed to ENR's better compatibility with ABS, which made the degradation of ABS/ENR blends more difficult [12]. These results are in good agreement with the FTIR data. The polarity of the epoxy and nitrile groups will increase the interaction and compatibility between the ENR and ABS mixtures. It is due to hydrogen bonds and van der Waals forces that are essential in establishing compatibility. However, with 50% ENR loading, the degradation temperature decreases slightly (385.7°C). It is attributed to the impact of a highly porous membrane and numerous beads on the fibre's surface that would affect thermal stability.

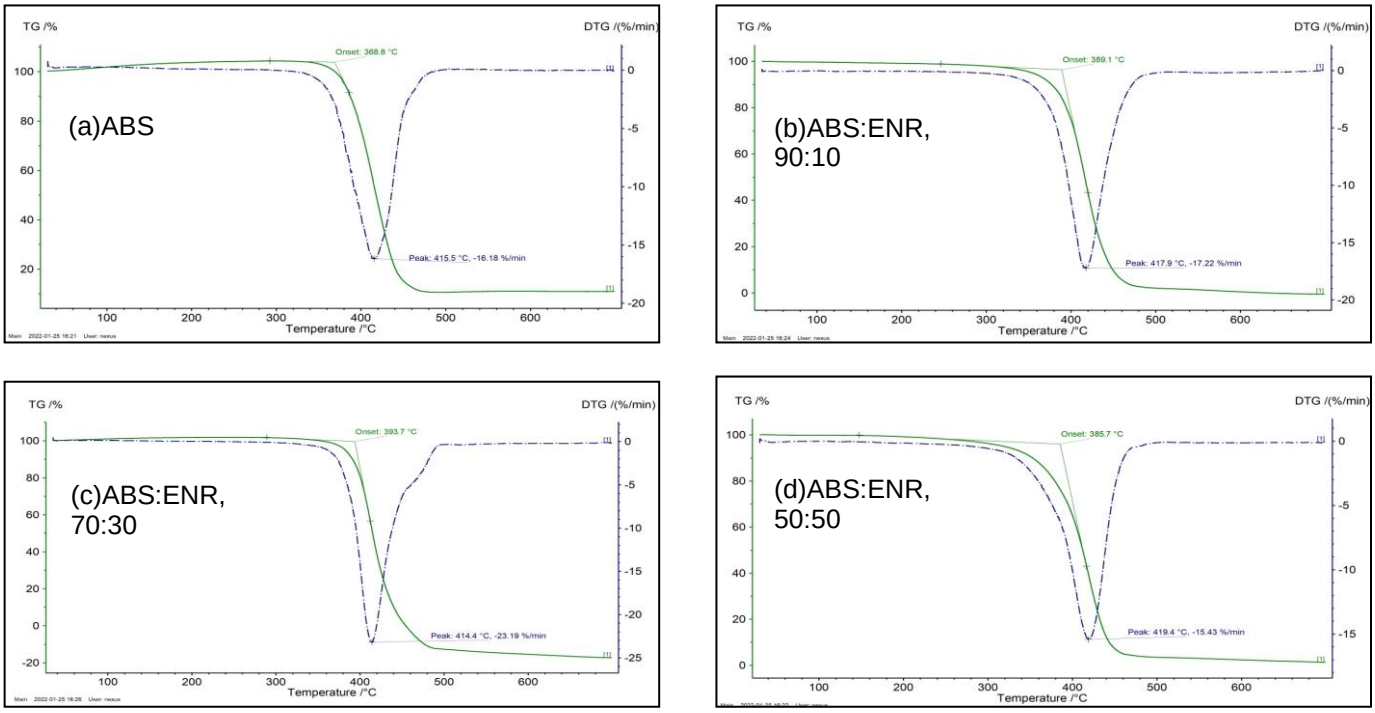

Figure 6. TGA curves for neat (a) ABS and ABS/ENR (b. 90:10, c. 70:30, d. 50:50).

4. CONCLUSIONS

The production of the ABS/ENR fibres was successful using the electrospinning process. FTIR indicated some interaction occurred between the ABS and ENR phases at a physical level. An increasing solution concentration generated morphological changes from beads to pure fibres. The findings revealed that the spinnable concentration of ABS/ENR is over 15%, and higher solution concentration enhances the creation of uniform fibres devoid of beads. There was an increase in the average diameter of the fibres as the polymer concentration increased (20% and 25%). Increasing the ENR ratio would lower viscosity and be proportionate to the diameter size production of electrospun fibres (~0.89µm). The increased conductivity at high voltage might increase the effect of electrostatic charge on the jet, forcing it to move quickly towards the screen collector and forming smooth fibres. An extension of the distance between the needle tip and the collector causes the advancing fibres to encounter larger stretching forces, notably in the whipping area, due to bending instabilities resulting in a drop in fibre diameters (1.02µm to 0.69µm). TGA studies revealed that ABS with ENR content has a higher degradation temperature than electrospun fibres that contain ABS only (~393.7°C).

ACKNOWLEDGMENTS

The authors would like to thank the Malaysia Ministry of Higher Education for sponsoring this work through Grant No. GUP-2019-007.

REFERENCES

[1] S. Nauman, L. Gilles, and H. F. Alharbi, "Post processing strategies for the enhancement of mechanical properties of ENMS (Electrospun nanofibrous membranes): A review," *Membranes*, vol. 11, no. 1, p. 39, 2021.

[2] K. C. Khulbe and T. Matsuura, "The advances of electrospun nanofibers in membrane technology," *J. Membrane Sci. Res.*, vol. 6, no. 3, pp. 251-268, 2020.

[3] Y. Liao *et al.*, "Progress in electrospun polymeric nanofibrous membranes for water treatment: Fabrication, modification and applications," *Prog. Polym. Sci.*, vol. 77, pp. 69-94, 2018.

[4] P. Kianfar *et al.*, "Enhancing properties and water resistance of PEO-based electrospun nanofibrous membranes by photo-crosslinking," *J. Mater. Sci.*, vol. 56, pp. 1879-1896, 2021.

[5] T. Subbiah *et al.*, "Electrospinning of nanofibers," *J. Appl. Polym. Sci.*, vol. 96, no. 2, pp. 557-569, 2005.

[6] L. Mascia *et al.*, "Fibres from blends of epoxidized natural rubber and polylactic acid by the electrospinning process: Compatibilization and surface texture," *Eur. Polym. J.*, vol. 87, pp. 241-254, 2017.

[7] S. Sithornkul and P. Threepopnatkul, "Morphology of electrospun natural rubber with acrylonitrile-butadiene-styrene," *Adv. Mater. Res.*, vol. 79, pp. 1583-1586, 2009.

[8] M. H. Othman, M. Mohamed, and I. Abdullah, "Electrospinning of PVC with natural rubber," in *AIP Conf. Proc.*, vol. 1571, no. 1, pp. 926-931, 2013.

[9] Y. Tertyshnaya *et al.*, "Electrospun Polylactide/Natural Rubber Fibers: Effect Natural Rubber Content on Fiber Morphology and Properties," *Polymers*, vol. 13, no. 14, p. 2232, 2021.

[10] S. Ibrahim, R. Daik, and I. Abdullah, "Functionalization of liquid natural rubber via oxidative degradation of natural rubber," *Polymers*, vol. 6, no. 12, pp. 2928-2941, 2014.

[11] A. Burkov *et al.*, "Structural features and properties' characterization of polylactic acid/natural rubber blends with epoxidized soybean oil," *Polymers*, vol. 13, no. 7, p. 1101, 2021.

[12] H. Kargarzadeh *et al.*, "Functionalized liquid natural rubber and liquid epoxidized natural rubber: A promising green toughening agent for polyester," *J. Appl. Polym. Sci.*, vol. 132, no. 3, 2015.

[13] Y. J. Chiu *et al.*, "Fabrication, morphology control, and electroless metal deposition of electrospun ABS fibers," *Macromol. Mater. Eng.*, vol. 301, no. 8, pp. 895-901, 2016.

[14] A. Calderon *et al.*, "Morphological characterization of electrospun zeolite-filled Acrylonitrile Butadiene Styrene fibrous membrane for low pressured CO2 adsorption," *Sustain. Environ. Res.*, vol. 24, no. 5, pp. 365-371, 2014.

[15] E. Moradi *et al.*, "Electrospun acrylonitrile butadiene styrene nanofiber film as an efficient nanosorbent for head space thin film microextraction of polycyclic aromatic hydrocarbons from water and urine samples," *Talanta*, vol. 205, p. 120080, 2019.

[16] H. O. Muhammad *et al.*, "Preparation of Non-Woven Fiber Mats by Mixture of PVC and Epoxidized Natural Rubber," *J. Nucl. Relat. Technol.*, vol. 11, no. 1, pp. 1-9, 2014.

[17] N. H. A. Azhar, H. M. Rasid, and S. F. M. Yusoff, "Epoxidation and hydroxylation of liquid natural rubber," *Sains Malaysiana*, vol. 46, no. 3, pp. 485-491, 2017.

[18] F. S. Kamelian *et al.*, "Preparation of acrylonitrile-butadiene-styrene membrane: Investigation of solvent/nonsolvent type and additive concentration," *Korean J. Chem. Eng.*, vol. 31, pp. 1399-1404, 2014.

[19] M. Mandegari and H. Fashandi, "Untapped potentials of acrylonitrile-butadiene-styrene/polyurethane (ABS/PU) blend membrane to purify dye wastewater," *J. Environ. Manage.*, vol. 197, pp. 464-475, 2017.

[20] J. G. Bokria and S. Schlick, "Spatial effects in the photodegradation of poly (acrylonitrile–butadiene–styrene): a study by ATR-FTIR," *Polymer*, vol. 43, no. 11, pp. 3239-3246, 2002.

[21] R. Arrigo *et al.*, "Effect of SiO2 particles on the relaxation dynamics of epoxidized natural rubber (ENR) in the melt state by time-resolved mechanical spectroscopy," *Polymers*, vol. 13, no. 2, p. 276, 2021.

[22] P. Saramolee, N. Lopattananon, and K. Sahakaro, "Preparation and some properties of modified natural rubber bearing grafted poly (methyl methacrylate) and epoxide groups," *Eur. Polym. J.*, vol. 56, pp. 1-10, 2014.

[23] T. Xu *et al.*, "Interfacial interaction between the epoxidized natural rubber and silica in natural rubber/silica composites," *Appl. Surf. Sci.*, vol. 328, pp. 306-313, 2015.

[24] E. Eastwood *et al.*, "Methods to improve the properties of polymer mixtures: optimizing intermolecular interactions and compatibilization," *Polymer*, vol. 46, no. 12, pp. 3957-3970, 2005.

[25] C. Mit-uppatham, M. Nithitanakul, and P. Supaphol, "Ultrafine electrospun polyamide-6 fibers: effect of solution conditions on morphology and average fiber diameter," *Macromol. Chem. Phys.*, vol. 205, no. 17, pp. 2327-2338, 2004.

[26] M. K. Selatile *et al.*, "Recent developments in polymeric electrospun nanofibrous membranes for seawater desalination," *RSC Adv.*, vol. 8, no. 66, pp. 37915-37938, 2018.

[27] T. Nuge *et al.*, "Characterization and optimization of the mechanical properties of electrospun gelatin nanofibrous scaffolds," *World J. Eng.*, vol. 17, no. 1, pp. 12-20, 2020.

[28] M. Aliabadi, "Effect of electrospinning parameters on the air filtration performance using electrospun polyamide-6 nanofibers," *Chem. Ind. Chem. Eng. Q.*, vol. 23, no. 4, pp. 441-446, 2017.

[29] A. Zulfi *et al.*, "The synthesis of nanofiber membranes from acrylonitrile butadiene styrene (ABS) waste using electrospinning for use as air filtration media," *RSC Adv.*, vol. 9, no. 53, pp. 30741-30751, 2019.

[30] J. H. Tan *et al.*, "Effects of epoxidized natural rubber as a compatibilizer on latex compounded natural rubber-clay nanocomposites," *J. Polym. Eng.*, vol. 37, no. 1, pp. 43-51, 2017.

[31] S. Tungprapa *et al.*, "Electrospun cellulose acetate fibers: effect of solvent system on morphology and fiber diameter," *Cellulose*, vol. 14, pp. 563-575, 2007.

[32] S. Huan *et al.*, "Effect of experimental parameters on morphological, mechanical and hydrophobic

properties of electrospun polystyrene fibers," *Materials*, vol. 8, no. 5, pp. 2718-2734, 2015.

[33] K. P. Matabola and R. M. Moutloali, "The influence of electrospinning parameters on the morphology and diameter of poly (vinyledene fluoride) nanofibers-effect of sodium chloride," *J. Mater. Sci.*, vol. 48, pp. 5475-5482, 2013.